Structure of molybdenum oxide clusters prepared in zeolite cages

Yasuaki Okamoto[1], Yasuhiro Kobayashi and Toshinobu Imanaka

Department of Chemical Engineering, Faculty of Engineering Science, Osaka University, Toyonaka, Osaka 560, Japan

Molybdenum hexacarbonyl entrapped in NaY zeolite was oxidized with molecular oxygen by UV-irradiation at room temperature or by thermal treatment at 343–373 K. Both oxidation procedures resulted in the identical molybdenum(VI) oxide; molybdenum dimer species (Mo–Mo distance: 0.321 nm). The Mo–Mo bonding of the oxide species was degraded on an evacuation at 673 K, while it was considerably stable in the presence of gaseous oxygen.

Keywords: Molybdenum oxide; molybdenum hexacarbonyl; zeolite; tungsten hexacarbonyl; EXAFS; XPS; photooxidation

1. Introduction

Uniform and well defined surface oxide species are anticipated to form when uniform supports and well characterized metal precursors are employed in the preparation of catalysts. Zeolites are widely appreciated as potential supports for these purposes because of their uniform, homogeneous crystalline structures having unique, ordered pore systems on a molecular level.

Many workers have investigated molybdenum hexacarbonyl $Mo(CO)_6$ encaged in cation exchanged X- and Y-type zeolites [1–4]. Vacuum decomposition of $Mo(CO)_6$ encapsulated in zeolite proceeds via various subcarbonyls $Mo(CO)_x$ ($x = 5, 4, 3$), finally producing Mo-metal. The decomposition rate strongly depends on the cation in zeolite, that is, the basic strength of the zeolite framework oxygen [2,3]. The intermediate subcarbonyl species are very reactive towards molecular oxygen. In the present study, we report the preparation of molybdenum oxides in zeolite using $Mo(CO)_6$ encapsulated therein by a photooxidation or thermal oxidation procedure. While this work was in progress, Ozin and coworkers [5,6] reported the structure of tungsten oxides prepared by photooxidation of $W(CO)_6$/NaY. Very recently, some results on $Mo(CO)_6$/NaY have appeared from

[1] To whom correspondence should be addressed.

their laboratory [7]. As shown below, the present results enrich the preparation chemistry of molybdenum oxides in zeolite cages.

2. Experimental

Zeolite NaY, $Na_{57}Al_{57}Si_{135}O_{384}$, was supplied by the Catalysis Society of Japan as a reference catalyst (JRC-Z-Y4.8). After evacuation ($<1 \times 10^{-5}$ Torr) at 673 K for 1.5 h, intermitted by an oxygen treatment (100 Torr for 0.5 h), the NaY zeolite in a quartz reactor was exposed to a $Mo(CO)_6$ (Strem Chemicals Inc.) vapor at room temperature for 16 h. The bottom of the reactor was made flat (2.8 cm in diameter) for UV-irradiation. Photooxidation of $Mo(CO)_6$/NaY (0.5 g) was conducted in an atmospheric oxygen flow predried by a zeolite trap at a methanol–dry ice temperature using a high pressure mercury lamp (Toshiba Lighting & Technology Corp., SHL-100UVQ; 75 W) with an H_2O filter (10 cm). The reactor was sometimes shaken during the photooxidation to equally irradiate the sample by mixing. When no further evolutions of CO and CO_2 were observed ($\sim$ 60 h), the reaction was assumed to be complete.

Thermal oxidation of $Mo(CO)_6$/NaY was carried out without irradiation using a closed circulation system (200 ml) at the oxygen pressure of 150 Torr and 343–373 K. The reactor was also shaken sometimes to ensure homogeneity of the sample. Complete oxidation of $Mo(CO)_6$ (0.5 g zeolite) took about 30 h at 358 K, but an additional oxygen treatment of several hours was applied for caution.

According to chemical analysis, the Mo-contents in both series of molybdenum oxide/NaY samples thus prepared were 1.2 ± 0.1 Mo atoms/supercage, about 60% of the full coverage of 2 Mo atoms/supercage [8,9]. As mentioned previously [10], this resulted from a preferential adsorption of $Mo(CO)_6$ in the outer layer of NaY lumps that were formed during the evacuation procedures. Similar observations were also reported by Tway and Apple [11].

The Mo K-edge EXAFS spectra for molybdenum oxide/zeolite systems thus prepared were measured at room temperature with the BL-10B instrument of the Photon Factory in the National Laboratory for High Energy Physics (KEK-PF) using synchrotron radiation. The EXAFS spectra were obtained without exposing the sample to air by using in situ EXAFS cell having Kapton windows. Data analysis was carried out using a plane wave approximation [12].

$Mo(CO)_6$ and $W(CO)_6$ (Strem Chemicals Inc.) encaged in the NaY were used for kinetic studies of the photooxidation process. The amount of zeolite charged in the reactor was 0.02 g in this case to well disperse the zeolite on the flat surface of the reactor bottom and to ensure homogeneous irradiation all over the sample. The amounts of CO and CO_2 evolved were measured by on line gas chromatography as a function of irradiation time. In these experiments with such small amounts of zeolite, the Mo- or W-contents incorporated into the zeolite were 2.0 ± 0.2 atoms/supercage, the saturation coverage, by chemical analysis.

3. Results and discussion

Shown in fig. 1 is the photooxidation behavior of $W(CO)_6$/NaY as a function of UV-irradiation time. Before irradiation, no evolution of CO or CO_2 was detected. The molar ratio of CO/CO_2 was 9–12 at 5 h irradiation, slightly decreasing with O_2 pressure (27–360 Torr). The predominant evolution of CO is contrary to the observations by Ozin and Ozkar [5] that the gaseous product of photooxidation is exclusively CO_2. This may arise from the differences in the irradiation light and its power (450 W high pressure Xe arc lamp [5] vs. 75 W high pressure Hg lamp). The evolution of CO in the present study is not due to a thermal decomposition process of $W(CO)_6$ adsorbed in zeolite (vide infra).

With $Mo(CO)_6$ encaged in NaY, a gradual thermal decarbonylation was observed to occur even at room temperature as revealed by the change in the sample color from pale yellow to yellow on evacuation, this rendering more precise analysis of the photooxidation process difficult. The CO/CO_2 molar ratios during the photooxidation of $Mo(CO)_6$/NaY, however, were about 15 as observed for the $W(CO)_6$/NaY systems.

Fig. 2 illustrates the effect of the wavelength upon the photooxidation rate which is calculated from the total amount of CO and CO_2 evolved (n) and the initial amount of CO (n_0). A linear correlation between $\ln(n_0 - n/n_0)$ and irradiation time indicates that the photooxidation process is first order with respect to the concentration of adsorbed $W(CO)_6$ in NaY zeolite. When light of wavelength <330 nm was cut off by using a filter (UV-37; Toshiba Glass Ltd.), the oxidation rate was

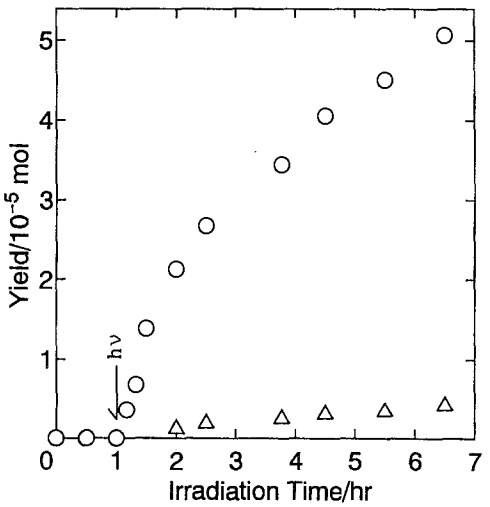

Fig. 1. Photooxidation of $W(CO)_6$ entrapped in NaY zeolite. Evolutions of CO (○) and CO_2 (△) are shown as a function of irradiation time. UV-irradiation started after 1 h.

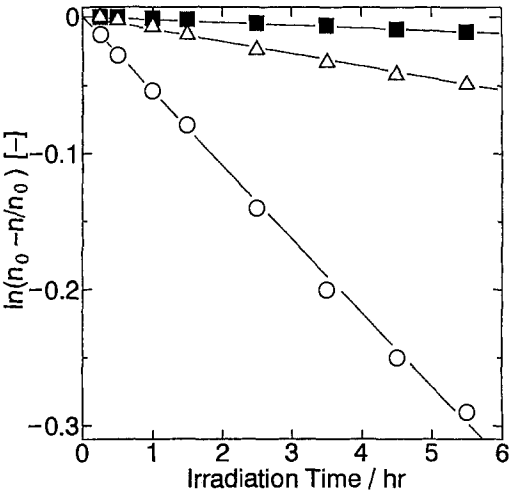

Fig. 2. Effect of irradiation light on the rate of photooxidation of $W(CO)_6$ encaged in NaY zeolite. (○) no filter, (△) <330 nm is filtered out, and (■) <400 nm is filtered out.

reduced to about one fifth of the original rate. No photooxidation was essentially observed when the sample was irradiated with light >400 nm (filter; Y-43, Toshiba Glass Ltd.). Simon et al. [13] have reported that $M(CO)_6$ (M = Cr, Mo, W) adsorbed on porous Vycor glass is photo-decomposed by irradiation with 312 or 350 nm light. Accordingly, it is concluded that the present photooxidation data represent a photo-induced oxidation reaction of $W(CO)_6$ with molecular oxygen rather than a thermal process. The first step of the reaction is a direct cleavage of the W–CO bond by irradiation, followed by an oxygen attack leading to successive W–CO bond cleavages and concomitant W–O and/or W=O bond formations.

With $Mo(CO)_6$, linear correlations similar to those in fig. 2 were obtained, although larger slopes were observed in the initial stage of the reaction. The initial enhanced evolution of CO is apparently due to a thermal decomposition of $Mo(CO)_6$ encaged in NaY before an exposure to O_2. Accordingly, $Mo(CO)_6$ and $W(CO)_6$/NaY are conjectured to show the identical reaction modes, except for the fact that part of $Mo(CO)_6$ is thermally oxidized during irradiation because of a lower thermal stability in the NaY zeolite cages.

The key step in the photooxidation is the photo-induced cleavage of the M–CO bond of $M(CO)_6$ (M = W, Mo). The M–CO bond breakings are also thermally initiated when $M(CO)_6$ is entrapped in zeolite. Fig. 3 depicts the temperature programmed decomposition (TPDE) profiles of $W(CO)_6$ and $Mo(CO)_6$ encaged in the NaY zeolite in a dynamic vacuum. It is evident that the decomposition rate is easily controlled by varying the temperature. It is anticipated that highly dispersed, well defined molybdenum oxide is provided thermally in a zeolite, when $Mo(CO)_6$ in zeolite is decomposed at 340–370 K in the presence of gaseous oxygen. It was found that thermal oxidations of $Mo(CO)_6$/NaY at 343–373 K caused evolution of

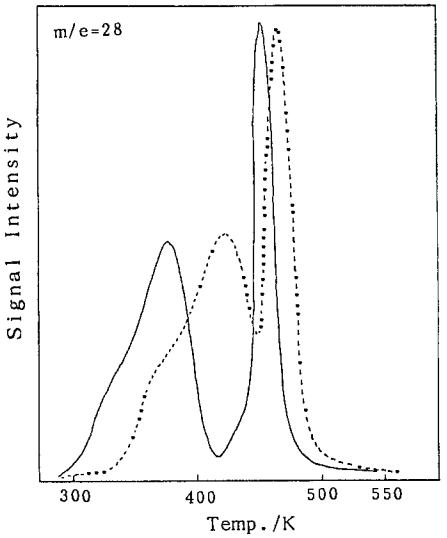

Fig. 3. Temperature programmed decomposition profiles of $Mo(CO)_6$ (solid line) and $W(CO)_6$ (dotted line) encaged in NaY zeolite. The rate of temperature increase; 2 K min^{-1}.

CO and CO_2 ($CO/CO_2 = 15$ at 358 K). The product molybdenum species was Mo(VI) oxide (Mo $3d_{5/2}$; 233.1 eV) as revealed by XPS measurements. The XP spectrum for the photooxidation products also indicated the formation of Mo(VI) (Md $3d_{5/2}$; 233.0 eV) oxide.

The Mo 3d/Si 2p XPS intensity ratios for the samples used in the kinetic experiments were consistent with the ratios expected from the chemical composition and atomic sensitivity factors, suggesting that molybdenum oxides are homogeneously dispersed in the cages of the NaY zeolite. High resolution TEM observations [14] clearly demonstrated no destruction of zeolite crystals in agreement with XRD results and showed no agglomeration of free molybdenum oxides outside the zeolite.

The structure of molybdenum oxides prepared in the NaY zeolite was studied by means of EXAFS. Fig. 4 illustrates Fourier transforms (FTs) of molybdenum oxides produced by photooxidation and thermal oxidation. The FTs for MoO_3, Na_2MoO_4, and $Mo(CO)_6$/NaY are also depicted for comparison. Both FTs for the molybdenum oxides prepared in NaY are very similar and consist of two peaks at 0.13 and 0.28 nm (not corrected for phase shift). The FT peak at 0.13 nm is unambiguously attributed to Mo–O bonds. On the other hand, the assignment of the FT peak at 0.28 nm to a Mo–Mo bonding is not straightforward, since back scattering from the oxygen atom in Mo–CO bond causes the FT peak at a close distance (0.27 nm, uncorrected) as shown in fig. 4. The FT peak at 0.28 nm could be reasonably curve-fitted by assuming either Mo–Mo bonding or Mo–CO bonding. However, the calculated bond length of 0.328 nm for the Mo–CO bonding is

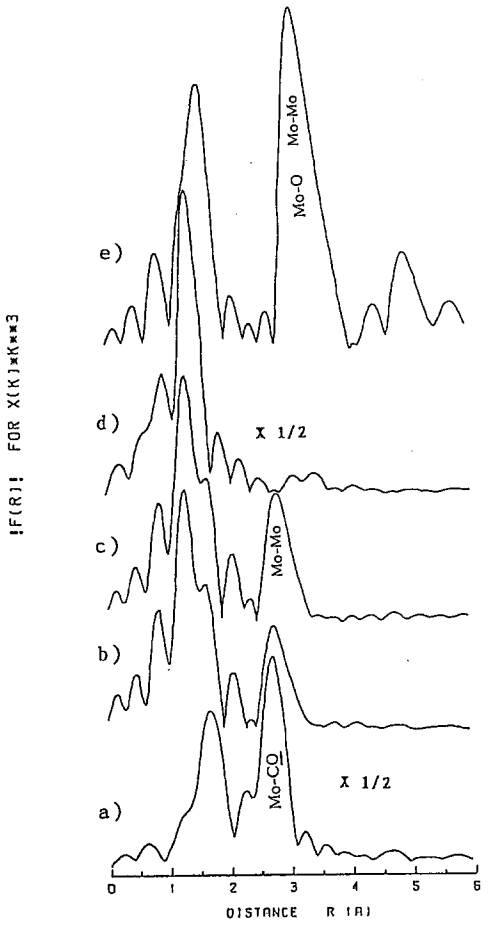

Fig. 4. Magnitude of the k^3-weighted Fourier transforms of $Mo(CO)_6$/NaY (a), molybdenum oxides in NaY zeolite fabricated by photooxidation (b) and thermal oxidation (373 K) (c), $Na_2MoO_4 \cdot 2H_2O$ (d), and MoO_3 (e).

not acceptable, since the bond length is considerably longer than that for $Mo(CO)_6$ (0.321 nm) in the NaY zeolite (table 1). The Mo–CO bond distance for Mo–subcarbonyl species is expected to be even shorter than that of $Mo(CO)_6$ because of increased back donation (e.g. 0.305–0.308 nm for $Mo(CO)_3$/NaY [10]). In addition, the findings that the FT peak remained, at least, partly intact at 673 K in the presence of gaseous oxygen entirely excludes the possibilities of the assignments of the peak to Mo–carbonyl species (vide infra). Consequently, the FT peak at 0.28 nm is concluded to be assigned to a Mo–Mo bonding, indicating the formation of molybdenum oxide clusters in zeolite cages rather than monomeric species.

The structural data derived from EXAFS analysis are summarized in table 2.

Table 1
Crystallographic data of reference compounds used for EXAFS analysis

Compound	Atom pair	CN[a]	R^b (nm)
$Na_2MoO_4 \cdot 2H_2O$	Mo–O	4	0.1772 [15]
MoS_2	Mo–Mo	6	0.316 [16]
$Mo(CO)_6$	Mo–C	6	0.2063 [17]
	Mo–CO	6	0.3208 [17]

[a] Coordination number.
[b] Bond distance.

The Mo–O region was reasonably curve-fitted only by assuming two Mo–O bondings. The shorter Mo–O bonds at 0.175 nm are ascribed to Mo=O double bonds, while the longer ones at 0.193 nm to Mo–O single bonds. The coordination number of the Mo–Mo bonding is close to unity, suggesting the formation of Mo_2O_6 dimer oxide species. The photo- and thermal oxidation procedures evidently provide oxides with the identical structure, suggesting the formation of a single stable species with a defined molecular structure. It is deemed that the structure of Mo–oxide dimer species emerging from the present EXAFS analysis is close to the structure proposed by Ozin et al. [5,6] for $(WO_3)_2$ encaged in zeolite. In addition, they have also shown by EXAFS that the structure of tungsten dimer species does not depend on the $W(CO)_6$ concentration in a NaY zeolite.

In contrast to the present EXAFS results, Jelinek et al. [7] reported a production of monomeric Mo-oxide species by photooxidation of $Mo(CO)_6$/NaY (450 W, high pressure Xe arc lamp). As mentioned above, the differences in the structure of the Mo-oxides are conjectured to reside in the differences in the reaction conditions. Under their photoreaction conditions, the oxidation was reported to com-

Table 2
Structural data as derived from EXAFS analysis[a]

Sample	Atom pair	CN	R (nm)	$\Delta\sigma^2$ (10^{-5} nm^2)	ΔE_0 (eV)
Mo-oxide/NaY(photo)	Mo–O	2.7	0.175	5.0	0.0
	Mo–O	3.2	0.193	7.9	−9.4
	Mo–Mo	0.7	0.320	0.0	−12.9
Mo-oxide/NaY(thermal, 373 K)	Mo–O	2.4	0.175	4.8	0.0
	Mo–O	2.7	0.193	7.7	−7.4
	Mo–Mo	0.8	0.322	−0.5	−7.7
$Mo(CO)_6$/NaY	Mo–C	6.3	0.207	0.6	0.1
	Mo–CO	5.7	0.322	0.0	0.1

[a] CN; coordination number, R; bond distance, $\Delta\sigma^2$; DW like factor, ΔE_0; inner potential.

plete within 1 h, contrary to ~ 50 h under the present conditions. These differences may also cause the different gaseous products, CO vs. CO_2.

Thermal stability of Mo-dimer species, which had been thermally prepared at 373 K, was examined in brief. When the sample was evacuated at 673 K for 2 h, it turned into brown in color, suggesting a partial reduction of Mo(VI). ESR measurements showed the appearance of signals attributable to Mo(V) at $g_{\perp} = 1.932$ and $g_{\parallel} = 1.910$. The FT for the molybdenum oxide/NaY treated in a vacuum at 673 K is depicted in fig. 5. The intensity of the FT peak at 0.28 nm due to the Mo–Mo bonding was significantly reduced, suggesting degradation of the molybdenum oxide dimer species to monomeric molybdenum oxide species or to disordered Mo-oxide clusters in the structure. On the other hand, the FT peak at 0.28 nm appears when the molybdenum oxide/NaY was heat-treated at 673 K in the presence of gaseous oxygen (180 Torr, white in color). Accordingly, it is concluded that the structure of the dimer species is considerably stable at 673 K in the presence of gaseous oxygen. More precise analyses of the EXAFS data are now under way.

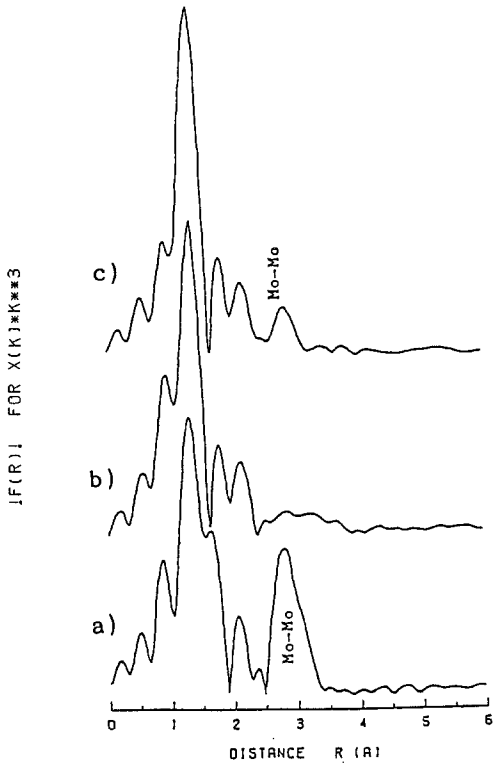

Fig. 5. Magnitude of k^3-weighted Fourier transforms of molybdenum oxide in NaY prepared by thermal oxidation (373 K). Fresh (a), evacuated at 673 K for 2 h (b), and heat-treated at 673 K for 2 h in the presence of gaseous oxygen (180 Torr) (c).

Acknowledgement

We thank Professor H. Kuroda and Professor N. Kosugi, who developed the EXAFS analysis programs, and Professor M. Nomura and staff of the Photon Factory, National Laboratory for High Energy Physics, for assistance in measuring EXAFS spectra (Proposal No. 92018).

References

[1] R.F. Howe, *Tailored Metal Catalysts*, ed. Y. Iwasawa (Reidel, Dordrecht, 1986) p. 141, and references cited therein.
[2] Y. Okamoto, A. Maezawa, H. Kane and T. Imanaka, J. Chem. Soc. Faraday Trans. I 84 (1988) 851.
[3] A. Maezawa, H. Kane, Y. Okamoto and T. Imanaka, Chem. Lett. (1988) 241;
Y. Okamoto, A. Maezawa, H. Kane and T. Imanaka, *Proc. 9th Int. Congr. on Catalysis*, Calgary 1988, eds. M.J. Phillips and M. Ternan (Chem. Inst. of Canada, Ottawa, 1988) p. 11.
[4] S. Ozkar, G.A. Ozin, K. Moller and T. Bein, J. Am. Chem. Soc. 112 (1990) 9575.
[5] G.A. Ozin and S. Ozkar, J. Phys. Chem. 94 (1990) 7556.
[6] K. Moller, T. Bein, S. Ozkar and G.A. Ozin, J. Phys. Chem. 95 (1991) 5276.
[7] R. Jelinek, S. Ozkar and G.A. Ozin, J. Phys. Chem. 96 (1992) 5949.
[8] T. Komatsu, S. Namba, T. Yashima, K. Domen and T. Onishi, J. Mol. Catal. 33 (1985) 345.
[9] Y. Yon-Sing and R.F. Howe, J. Chem. Soc. Faraday Trans. I 82 (1986) 2887.
[10] Y. Okamoto, T. Imanaka, K. Asakura and Y. Iwasawa, J. Phys. Chem. 95 (1991) 3700.
[11] C.C. Tway and T.M. Apple, Inorg. Chem. 31 (1992) 2885.
[12] M. Nomura, KEK Report (1985) 7.
[13] R.C. Simon, E.A. Mendova and H.D. Gafney, Inorg. Chem. 27 (1988) 2733.
[14] O. Terasaki, personal communications.
[15] K. Matsumoto, A. Kobayashi and Y. Sakai, Bull. Chem. Soc. Japan 48 (1975) 1009.
[16] R.G. Dickinson and L. Pauling, J. Am. Chem. Soc. 45 (1923) 1466.
[17] A. Whitaker and J.W. Jeffery, Acta Cryst. 23 (1967) 977.